https://doi.org/10.17221/148/2021-SWR

Construction and calibration of a portable rain simulator designed for the in situ research of soil resistance to erosion

Nikola Živanović[1], Vukašin RonČević[1], Marko Spasić[2], Stevan Ćorluka[3], Siniša Polovina[1]*

[1]*Ecological Engineering for Soil and Water Resource Protection, Faculty of Forestry, University of Belgrade, Belgrade, Serbia*
[2]*Faculty of Agrobiology, Food and Natural Resources, Czech University of Life Sciences Prague, Prague, Czech Republic*
[3]*Mining Institute Belgrade, Belgrade, Serbia*

**Corresponding author: nikola.zivanovic@sfb.bg.ac.rs*

Citation: Živanović N., Rončević V., Spasić M., Ćorluka S., Polovina S. (2022): Construction and calibration of a portable rain simulator designed for the in situ research of soil resistance to erosion. Soil & Water Res.

Abstract: Land degradation caused by erosion processes is a widespread global problem. Rain simulators are one of the tools often used to determine the resistance of soils to erosion processes. The aim of this publication is to present the process of the construction and calibration of a small, portable field simulator which would be implemented in research studies designed to determine the changes in the soils' shear strength parameters in forested areas (*in situ*) caused by a change in soil moisture content achieved by the rain simulation. The constructed simulator consists of a metal frame, sprayers (with specific nozzles), a sediment funnel/tray made of metal, water and a sediment collector unit, a water tank and pump, and a set of rubber hoses, manometer, valves, reducers, adapters and other supplementary equipment. The calibration was carried out by using the pluviometric method. The choice of nozzles was based on the criteria of low water consumption (losses), the Christiansen uniformity coefficient (CU) and the possibility of achieving specific downpour intensities for the investigated area. The further calibration of the device consisted of determining the raindrop diameter and the distribution of the rainfall when the simulator is positioned on the slopes (7° and 15°). The achieved rain intensity was 1.7–1.9 mm/min, with a CU of 92.23–93.70% for the raindrop diameters (D_{50}) equal to 1.2 mm. The kinetic energy of the simulated rain (*Ke*) was $2.82 \cdot 10^{-6}$ J. The constructed simulator proved itself to be in accordance with all of the given criteria, and it can successfully be implemented in research studies aimed at determining the resistance of forest soils to erosion processes, infiltration, and sediment yield.

Keywords: field rain simulator; raindrop diameter; raindrop distribution; soil erosion

Globally speaking, erosion is the most widespread form of soil degradation, and is interconnected with various other environmental and social problems (Konz et al. 2010; Panagos et al. 2015; Montanarella et al. 2016; Guerra et al. 2017; Zhang et al. 2019a; Borrelli et al. 2020; Kavian et al. 2020). Although some developed strategies have been successful in reducing the devastating effect of erosion, there is much more to be done, since soil erosion rates are still much greater (by a factor of 1.6 in the EU) than the

Supported by the Ministry of Education, Science and Technological Development of Republic of Serbia, Project NTPR 33044.

https://doi.org/10.17221/148/2021-SWR

soil formation rate, causing a total annual soil loss of 2.46 t/ha (Panagos et al. 2015). Considering these values are such as they are in the EU countries, which can generally be considered developed, the situation is much worse on a global scale. According to Blinkov (2015), the Western Balkan countries have an erosion intensity of 656 m^3/ha (approximately 6.56 t/ha). The average soil loss for Belgrade (the capital of Serbia) was 3.63 t/ha in 2019 (Polovina et al. 2021).

The suppression and mitigation of soil erosion process relies on choosing appropriate soil conservation strategies. On the other hand, this requires a fundamental understanding of the soil erosion process (Morgan 2009). Research on erosion processes are mainly undertaken in agricultural areas, while they are much less looked into in mountainous and forested regions (Konz et al. 2010; Borrelli et al. 2017; Poesen 2018). Erosion processes in forests significantly reduce or completely disrupt the production potential of the forest ecosystem (Neiuwenhuis 200). According to FAO (2011), forested areas are basically more sensitive to degradation caused by soil erosion than most agricultural surfaces, meadows and pastures. Kašanin-Grubin et al. (2021) pointed out that a dramatic reduction in the resistance of forest soil to erosion due to climate change and forest management can be expected.

Experimental research is becoming more and more significant in understanding and assessing the soil erosion processes and their mechanisms (Hudson 1993; Guo et al. 2020). The development, construction and calibration of rain simulators, as well as their first applications, started in the early 20th century (Cerdà 1999; Newesely et al. 2015). Rain simulators are widely used tools in the research of hydrological processes, which also include soil and rain interactions, soil erosion, surface runoff and infiltration. According to (Meyer & Harmon 1979), acquiring data needed to assess soil erosion processes tend to be much faster when a rain simulator is applied in comparison to waiting for natural rain occurrences. Using rain simulators for different purposes requires different properties of the apparatus, which has led to a lack of standardised methodology in the construction of simulators, and further, to develop various types of rain simulators, each corresponding to the individual needs that it was constructed for (Wilson et al. 2014). According to Lora et al. (2016), due to the mentioned lack of standards, and the specific requirements of each research, researchers often have to develop their own designs to suit their needs.

Generally, rain simulators can be divided into two groups – field (portable) presented in the papers by Meyer and Harmon (1979), Torri et al. (1994), Cerdà et al. (1997), Johansen et al. (2001), Holden and Burt (2002), Boix-Fayos et al. (2006), Clarke and Walsh (2007), Abudi et al. (2012), Parsakhoo et al. (2012), Dong et al. (2012), Wilson et al. (2014), Cao et al. (2015), Newesely et al. (2015), Zemke (2016), Polyakov et al. (2018), Vergni et al. (2018), Boulange et al. (2019), Kavian et al. (2019), Zemke et al. (2019) and laboratory (non-portable) simulators presented in the papers by Bryan (1974), Misra and Rose (1995), Zhang et al. (2019 b), Mhaske et al. (2019), Kavian et al. (2020), Qiu et al. (2021). Apart from that, they can be classified based on the way the drops are formed, into gravitational and pressurised simulators. With gravitational ones, raindrops are formed by free-fall after they exit the simulator tubes, which can vary in diameter. Pressurised simulators can be further divided into two groups, based on whether the stream is directed upwards (and the drops are formed gravitationally) or downwards (where the drops are formed by breaking or disrupting the stream) (Corona et al. 2013; Yakubu & Yusop 2017).

Iserloh (2012) pointed out the advantages of small, portable simulators compared to big ones, which can be reflected in the possibility of performing experiments on various specific surfaces with multiple repetitions, as well as being easier to handle and control the overall conditions of the experiment. Rain simulators remain a valuable tool, particularly in cases of downpours, or in extreme rain occurrence research, which would be almost unimaginable without them (Dunkerley 2008).

Research which has comprised the use of rain simulators has been performed in Serbia by several authors – Gavrilović (1972), Radić (1981) and Gabrić (2014), but these experiments have all been performed in laboratories. Field rain simulators for soil erosion process research have rarely been used both in Serbia and abroad, mostly due to the complexity of the experiment set-up in field conditions.

Any further development of rain simulators should address the water losses, raindrop diameter, distribution of the simulated rain, as well as the experimental repeatability, overall control and conditions during the operation of the simulator (Iserloh et al. 2013).

Understanding the ratio of the soil moisture content (which can vary significantly between and during downpour events) and the critical shear pressures is very important, especially when considering the

https://doi.org/10.17221/148/2021-SWR

significance the soil moisture has on the runoff formation and soil erosion (Singh & Thompson 2016).

The general idea of the experiment that this simulator has been constructed for is based on research into the influence of the moisture content changes of the surface soil layer on the shear strength and penetration resistance of forested area soils. Therefore, the main purpose of this paper is to present a detailed description of the design and calibration of a portable rain simulator as well as to draw conclusions about the fulfilment conditions having the idea of the experiment in mind.

MATERIAL AND METHODS

Material. The research area is located in the southern, hilly part of Belgrade (Serbia), in a forested area vegetated by a degraded Hungarian oak and Turkey oak (Quercetum frainetto-cerris) forest, where a significant area has been affected by landslides and gullies, initially caused by piping erosion. The geological substrate is made out of loess. Pedologically speaking, soils with a noticeable lessivage process are represented. The climate is moderately continental, with an average annual temperature of 12.47 °C and an annual rainfall of 691.89 mm. After the extreme rains that caused major floods in Serbia in 2014, the management of the forest had reported increased erosion and damage caused by it. During this rainfall occurrence, a daily rainfall maximum of 107.9 mm was reached (RHSS 2014).

Methods. For the purpose of this experimental research, the simulated rainfall should correspond to a downpour in intensity and duration. Downpour rains usually last between 6 and 15 min (Jevtić 1988). According to Milosavljević (1949) and Jevtić (1988), the rainfall intensity usually ranges around 1.67 and 1.70 mm/min, respectively. In a research based on data from 1946–2006, about strong, short rainfalls from a meteorological station in Belgrade-Vračar undertaken by Radić and Pavlović (2015), it was interpreted that the intensity was around 2.5 mm/min, for an average rainfall event of 10 min, and with a return period of 100 years. According to the same source, the maximum average values for Serbia, in general (for a rainfall episode of 10 min), are somewhere around 1.2 mm/min.

The simulator should provide the expected rain intensity of the actual locality where it is positioned, without excessive losses. The criteria that the constructed rain simulator is supposed to fulfil mainly correspond to the terms considered essential by Iserloh et al. (2012) for a small portable simulator: being portable, being easy to handle, efficient in terms of water consumption, having a homogenous intensity and coverage of the simulated rain during the experiment and the repeatability of the experiment under the same conditions. Besides that, it needs to have a surface area large enough for sample collection.

Determination of simulated rainfall intensity, spatial distribution and water losses. The calibration took place in an enclosed area, in order to eliminate the influence of wind. In order to determine the intensity of the simulated rainfall, its spatial distribution and water losses, a pluviometric method was used (Sangüesa et al. 2010; Parsakhoo et al. 2012; Iserloh et al. 2013; Mhaske et al. 2019). The rain simulation experiment was performed in 10-minute intervals per nozzle type for three nozzle types (Rain Bird type 6 Series VAN (6V), 8 series HE-VAN (8HV) (Rain Bird, USA), and Hunter A10 (A10) (Hunter, USA)), in order to determine the applicability of the nozzles based on the given criteria. The slope was 0°, and there were three measurement repetitions for each. Apart from that, there were three separate measurement repetitions for each slope setting (7° and 15°) of the 8HV type nozzle, after the nozzle had been chosen for further use based on the criteria: the amount of water used from the reservoir, the total amount of water which fell on the area of the simulator, the water losses, the spray radius and the rainfall uniformity values. This was achieved by positioning 225 micro-pluviometers made from plastic beverage cups. These pluviometers were positioned in a Styrofoam frame (dimensions 150 × 150 × 3 cm), which had rows of circular openings for the micro-pluviometers inside them. The distance from the centres of the opening was 10 cm, whereas the pluviometers positioned next to the metal frame had their centres 5 cm from the frame. The diameter of each pluviometer is 6.5 cm. The Styrofoam frame was positioned to be parallel to the lower frame base, thus representing the experimented soil on the terrain. The exact amount of collected water for each of the 225 pluviometers was determined by using a calibrated measuring cylinder. After each of the experiments, the used amount of water was calculated based on the changes in the water level of the water reservoir of known dimensions.

The uniformity of the simulated rainfall is expressed via the Christiansen uniformity coefficient (CU) (Christiansen 1942; Sangüesa et al. 2010; Parsakhoo

https://doi.org/10.17221/148/2021-SWR

et al. 2012; Iserloh et al. 2013; Mhaske et al. 2019), which is derived from Equation (1). The more uniform the rainfall, the closer the CU is to 100% (Abudi et al. 2012; Boulange et al. 2019).

$$CU = 1 - \frac{\sum_{i=1}^{n} \times |R_i - M|}{n \times M} \quad (1)$$

where:
CU – Christiansen uniformity coefficient (%);
R_i – amount of water in each pluviometer (mm);
M – mean amount of water in all the pluviometers (mm);
n – the number of the pluviometers.

The uniformity of the simulated rainfall was used to determine the sampling zone with a CU criterion over 90%.

Raindrop diameter determination. The raindrop size determination was performed by using the methodology suggested by Bentley in 1904 (Kathiravelu et al. 2016; Mhaske et al. 2019). Five dishes with their corresponding lids (23 cm in diameter) were positioned in the simulator area. Flour was levelled to a 1.5 cm thick layer in the dishes. After this was set up, the rain simulator was turned on, the lids for each dish were removed for 2–3 s, thus subjecting the flour in the dishes to the simulated rain, and then the lids were put back on. The flour was air dried in an oven for 24 h at the temperature of 105 °C, and was then sieved through a series of sieves with dimensions 3.0, 2.0, 1.4, 1.25, 1.0, 0.70 and 0.5 mm. This experiment was repeated twice. Based on the measured mass ratios, the raindrop diameter curve was drawn.

Raindrop kinetic energy determination. The kinetic energy of the raindrop (*Ke*) was determined by using Equation (2) suggested by Wischmeier and Smith in 1958 (Morgan 2009; Meshesha et al. 2019).

$$Ke = \frac{1}{2} \times m \times v^2 \quad (2)$$

where:
Ke – kinetic energy of the raindrop (J);
m – raindrop mass (kg);
v – raindrop velocity (m/s).

RESULTS

System design. The portable rain simulator designed in this research is comprised of: (1) a metal frame, (2) sprayers (with specific nozzles), (3) a metal sediment funnel/tray, (4) a water and sediment collector unit, (5) a set of rubber hoses with a manometer, valves, reducers, adapters and other supplementary equipment, (6) a water pump, and (7) a water tank. This design is graphically depicted in Figure 2.

(1) The metal frame is constructed in a way that it provides the proper positioning of the sprayers attached to it, and limits the area of the soil surface used in the experiment (Figure 2). It is comprised of 4 metal elements, 8 sprayer attachment stands, 12 bolts and 12 nuts. The metal elements are made from welded, interconnected iron profiles (dimensions 1.5 × 1.5 cm) and galvanised sheet metal sides. The metal elements differ amongst each other, and are thus classified in 3 categories (Figure 1). A type A element is one being positioned downwards (the side where the water and sediment are collected at). A type B element is parallel to type A, and is positioned at the uphill side. The type C elements (2×) are positioned as the lateral sides of the frame, perpendicular to A and B, and parallel to each other. These elements are connected to each other by 4 bolts and nuts which pass through pre-drilled holes in the corners of the elements and the metal plates with dimensions of 15.0 × 4.0 cm. Two plastic sprayer

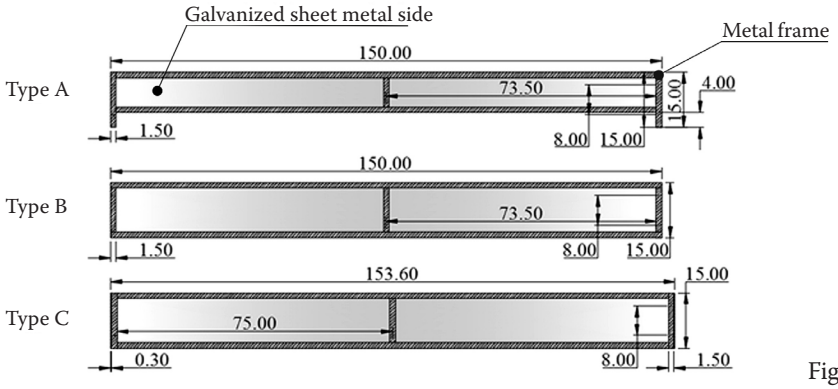

Figure 1. Dimensions of the metal elements

https://doi.org/10.17221/148/2021-SWR

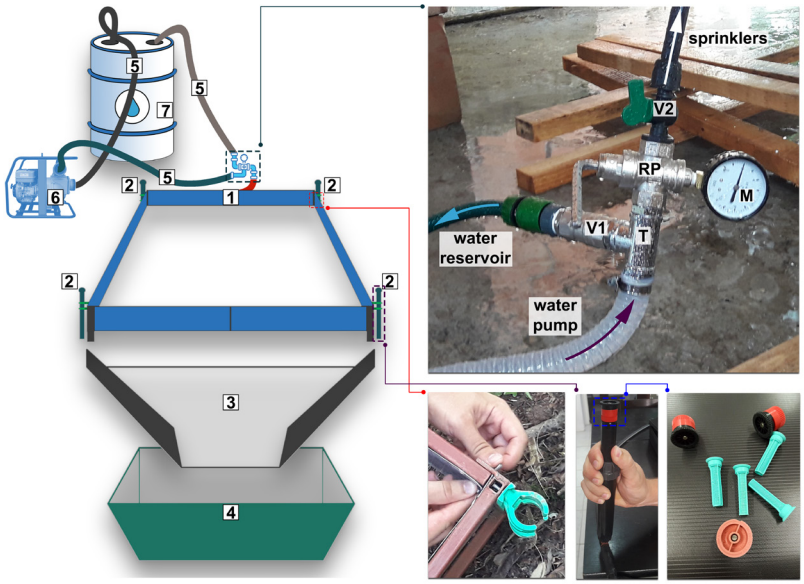

Figure 2. Design of the field rain simulator: a metal frame (1), sprayers (with specific nozzles) (2), a metal sediment funnel/tray (3), a water and sediment collector unit (4), a set of rubber hoses with a manometer, valves, reducers, adapters and other supplementary equipment (5), a water pump (6), and a water tank (7)

stands are attached on each of the type C element's ends. Once assembled in the specified way, the frame forms a solid construction, with an internal surface area of 2.25 m^2.

(2) The sprayers and nozzles were chosen according to the already determined research requirements, by analysing the specifications given in the manufacturer's catalogue (available at www.hunterindustries.com and www.rainbird.com) and their further calibration. The sprayers are positioned in the plastic stands at the corners of the metal frame, so that all of the sprayer housings are at the same height. The chosen model, "Rain Bird pop up US400", pops up 10 cm above the housing at the pressure of around 150 kPa (1.5 bar), and a water spray which is directed upwards commences. Thus, the drops are gravitationally formed. The nozzles chosen for this simulator are the Rain Bird type 6 Series VAN (6V), 8 series HE-VAN (8HV), and Hunter A10. The sprayers and nozzles have angle adjustments which can vary from 0 to 360°. For this particular research, the spraying angle is fixed at 90°, so that the simulated rainfall is directed towards the research area within the frame borders.

(3) The sediment funnel/tray is made of 3.0 mm thick galvanised sheet metal, has a trapezoidal shape (base lengths B1 = 152.0 and B2 = 60.0 cm), and its sides are bent upwards (height h = 40.0 cm) in order to avoid water and sediment losses. Its function is to transport the water and sediment from the metal frame to the sediment collector unit. It is positioned right below the type A element of the metal frame, and should be dug into the ground, in order to avoid water and sediment losses.

(4) The water and sediment collector unit is a plastic vessel with appropriate dimensions which is used to collect the water and sediment which pass through the sediment funnel. It should also be dug into the ground in order to establish the downward movement of the water and sediment from the sediment funnel/tray. After the experiment is finished, the contents of the collector unit are transferred to other sealed vessels and are transported for further lab analyses.

(5) A set of rubber hoses and some supplementary equipment are used for transferring the water from the water reservoir to the sprayers with a water pump. Reinforced rubber hoses with diameters of 2.54 and 1.27 cm are used, along with a suction head, a T-joint, manometer with a pressure reducer, valve connectors, and various clamps.

(6) The water pump chosen for this experiment is a gasoline, 4-stroke, one piston, internal combustion Villager WP 8 P (Villager, Slovenia). It is air cooled, has an engine displacement of 97.7 cm^3 and produces 1 kW of power. According to the specifications sheet, its maximum flow rate is 6 m^3/h and the maximum pressure is 200 kPa (2 bar).

https://doi.org/10.17221/148/2021-SWR

(7) The water reservoir can vary in volume, depending on the logistics and water availability at the experiment location, but, in order for the experiment to be performed, it should not be smaller than 120 L. The water in the reservoir should be clean, and special attention should be paid to preventing contaminating the water with leaves, branches or any other impurities which could lead to the water pump or sprayer filter malfunctioning.

System functioning. The water should be transferred from the water reservoir to the sprayers through a system of rubber hoses and supplementary equipment. There is a filter with a suction head fitted to the side of the rubber hose which leads from the reservoir. This filter prevents large sized impurities from getting inside the system. The water pump pushes the water through the 2.54 cm hose to the T-joint. On one side of the T-joint (T), a pressure reducer (RP) with a manometer (M) is attached, whereas on the other hose, there is a connector with a valve (V1). Through the 2.54 cm hose that is attached to the valve (V1), excessive water is pumped back to the water reservoir. There is another hose (1.27 cm in diameter) attached to the pressure reducer (RP) via a second valve (V2), which further leads water directly to the sprinklers (Rain Bird SBE-050 and SB-TEE, Rain Bird, USA), which are connected to the hose with clamps. The hoses that lead from the pressure reducer are positioned symmetrically to the pressure reducer, thus providing roughly constant pressure in all of the sprinklers (Figure 2).

Valve V2 provides an almost instant start to the spraying process, once the pump is turned on and the valve is opened. Pressure regulation is achieved by utilising the connector with the attached valve V1. This design also protects the system from sudden pressure changes, by returning the successive water back to the reservoir. The rubber hoses are attached to the pump and the T-joint by clamps, whereas the connectors are attached to the valves with appropriate fittings and seals. At the joints, the system is further protected by using Teflon tape. Apart from the valve, the pressure can be additionally controlled by controlling the throttle of the water pump. The entire system of hoses and sprinklers can be fully disassembled and reassembled again multiple times. The rainfall simulator during field operation is presented in Figure 3.

Due to the specific requirements of the research, a work pressure of 200 kPa (2 bar) was chosen. This pressure is read on the manometer, and can be considered constant throughout the whole system.

Rainfall intensity, spatial distribution and water losses. After assembling all the elements, the simulator system calibration was performed by establishing the intensity of the simulated rainfall, water losses, spatial distribution of the simulated rainfall and the raindrop diameters.

Based on the measurements performed, it was determined that during the experimental duration of 10 min, by using the nozzle types 6V, 8HV and A10, the water amount used from the reservoir was 60.3, 48.0 and 134.0 L, respectively. However, it was calculated that the total amount of water which fell on the area of the simulator was 57.4, 37.4 and 38 L, respectively. Having in mind that the system itself had no water losses, these losses can be explained as the water which fell beyond the boundaries of the metal frame. For the 6V, 8HV and A10nozzle types, the water losses were 4.81%, 22.08% and 71.64%, respectively. The spatial distribution of the water levels for all three nozzle types is graphically presented in Figure 4.

Considering that, with a test pressure of 200 kPa (2 bar), all three nozzle types had a sufficiently greater spray radius than was required, the spraying radius was reduced, by tightening the nozzle adjustment

Figure 3. The rainfall simulator during filed operation

https://doi.org/10.17221/148/2021-SWR

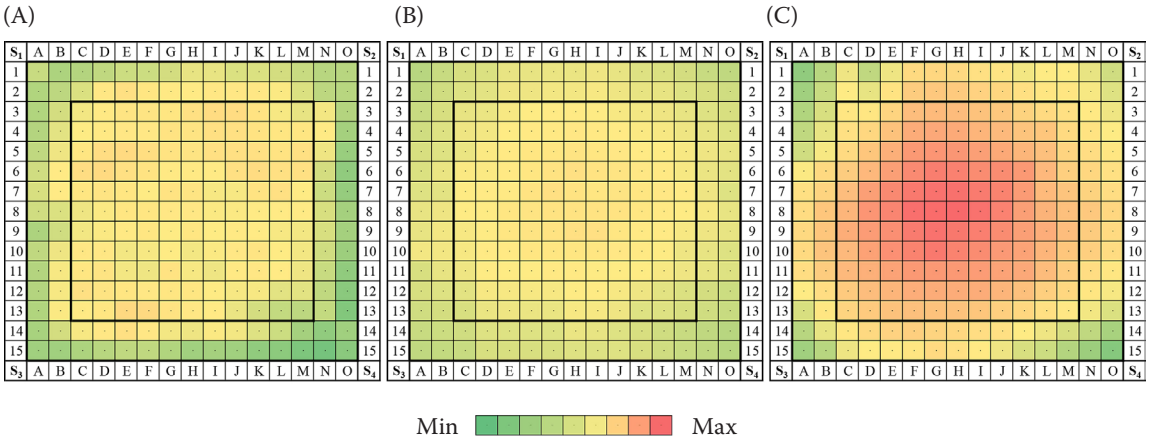

Figure 4. Spatial distribution of the water amounts from the 6V (A), 8HV (B) and A10 (C) sprayers at a slope angle of 0°

screw (according to catalogue specifications, this way, it is possible to reduce the spraying radius by up to 25%). There is a 1.8 m diameter in overlapping of the sprayer streams of the 8HV nozzle.

Uniformity of the simulated rainfall. The values of the rainfall uniformity for all three nozzle types are presented in Table 1. The A10 nozzle type proved to have the best CU value, followed by the 8HV, and 6V types for the whole tested area. Considering the water losses and uniformity coefficient values which were described earlier, the further calibration of the simulator was continued by using the 8HV nozzle. With this set-up, the rain simulation experiment was repeated with the same duration and number of repetitions as before, but with the slope angles changed to 7° and 15°. In these two instances, with 47 L of consumed water for both slopes, the water losses were 20.43% and 32.13%, respectively.

Figure 5 shows spatial distribution of the simulated rainfall, which was based on the measurement of the amount of water in the pluviometers. The presented distribution refers to the 8HV nozzle, for three different slope angles (0°, 7° and 15°). The sampling zone (dimensions 1.1 × 1.1 m, surface area 1.21 m^2), which has a uniformity coefficient greater than 90%, was marked in the figure. This zone was positioned in the centre of the frame for the experiments with

Table 1. Christiansen uniformity coefficient (CU) values for all three nozzle types, with additional values for the 7° and 15° slope of the 8HV nozzle

CU	6V	A10	8HV		
	0°	0°	0°	7°	15°
$CU_{2.25}$	72.98	91.06	83.01	79.65	73.93
$CU_{1.21}$	82.19	94.65	93.70	92.23	92.87

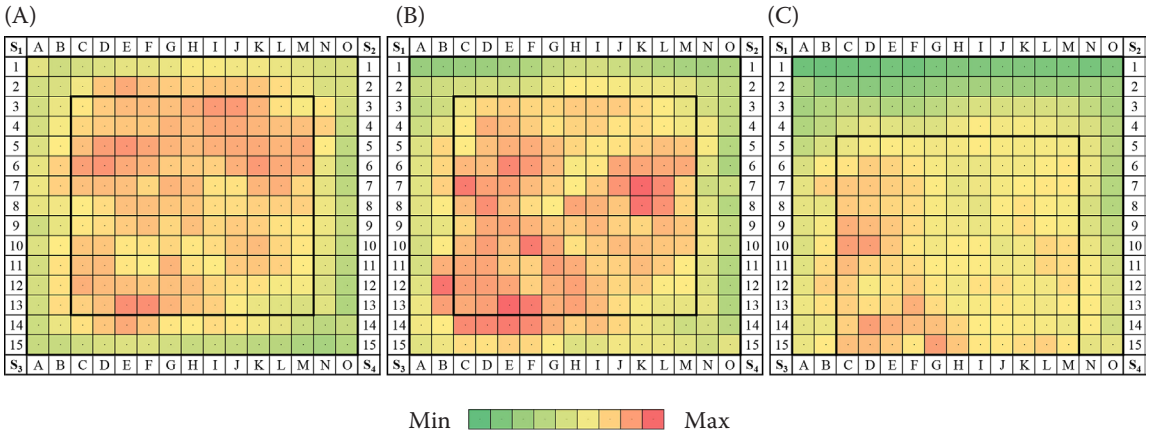

Figure 5. Spatial distribution of the simulated rainfall on the entire surface area (2.25 m^2), as well as in the marked sampling zone (1.21 m^2), for the 8HV nozzle type on the 0° (A), 7° (B) and 15° (C) slopes

https://doi.org/10.17221/148/2021-SWR

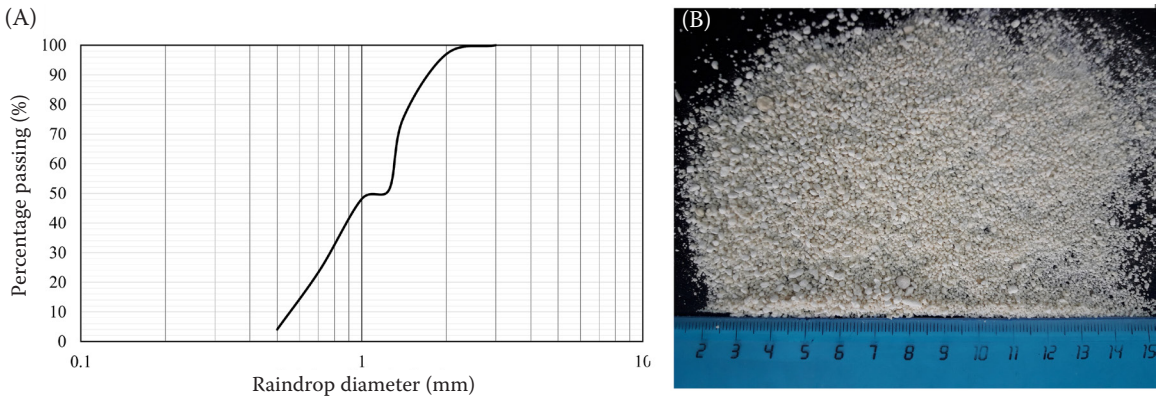

Figure 6. Raindrop diameter size distribution curve (A) and raindrop diameter determination by the flour method (B)

0° and 7° slope, and in the experiment with 15° slope, the zone was positioned towards the A element of the metal frame. The CU values for this marked zone varied between 92.23% and 93.70%. This zone was marked for the purpose of taking samples with the greatest uniformity amongst each other, and was also dimensioned with having a sufficient number of samples in mind.

Raindrop diameter. Based on the measured mass ratios, a raindrop diameter curve was drawn. The results show that the average raindrop diameter D_{50} is equal to 1.2 mm. For all five dishes and both repetitions, the ratios of the diameters were similar. The raindrop diameter sizes obtained by using the flour method are visible in Figure 6.

Raindrop kinetic energy. The calculation of the kinetic energy was performed based on a rainfall intensity of I = 1.9 mm/min and an average raindrop diameter of D_{50} = 1.20 mm. The raindrop velocity was derived from the numerical model proposed by Boxel (1997). According to this model, for the mentioned diameter and height (h = 0.5 m), the rainfall velocity is 2.50 m/s.

The raindrop energy, Ke, is thus equal to Ke = 2.82 10^{-6} J. The overall kinetic energy of the raindrops expressed through the height is Ke_{mm} = 3.12 J/m/mm. The overall kinetic energy expressed in time is equal to Ke_h = 355.35 J/m/h, or $Ke_{10\ min}$ = 59.23 J/m for the duration of a 10 min experiment.

DISCUSSION

The chosen rain simulator dimensions (1.5 × 1.5 m), with a surface area of 2.25 m^2 were based on two limiting factors: on one hand, the limitations which derive from the minimal surface area required to perform the experiment, and on the other, the maximum size of the metal frame elements and the ability to successfully transport them in a passenger car. According to Agassi and Bradford (1999), the area for field experiments should be more or less square shaped, with side (length and width) ratio being close to 1.

By utilising this simulator design, a rainfall intensity of 1.7 to 1.9 mm/min (102.0–114.0 mm/h) can be achieved on the test surface in which soil samples are to be taken from, depending on the slope angle in which the simulator is positioned (Table 2). The occurrence of rainfall which results in a water column greater than 0.5 mm/min is considered a downpour. Unlike common rainfall, which is characterised by longer periods of a lower rain intensity, downpours are specific for their short duration and heavy intensity (Jevtić 1978).

The constructed simulator was designed to provide a rainfall intensity which corresponds to the downpour intensity characteristic of the area (around 1.7 mm/min for durations of 6–15 min). The annual rainfall intensity maximum of a 15 min rain for many meteorological stations across Europe, for a one-year return period, varies between 40–44 mm/h, or 10–11 mm per 15 min (Rauch & De Toffol 2006).

Table 2. Rainfall intensity (I) accomplished on the tested surface, for different nozzle types on various slopes

Nozzle type	Slope (°)	$I_{2.25}$	$I_{1.21}$
		(mm/min)	
6V	0	2.6	3.1
A10	0	1.7	1.8
8HV	0	1.7	1.9
	7	1.7	1.9
	15	1.4	1.7

https://doi.org/10.17221/148/2021-SWR

Dunkerley (2008) stated that simulated rainfall intensity values of 60–100 mm/h are the most commonly used ones in experiments and scientific publications.

Based on the methodology used, and repeated research cycles at the same location, it can be presumed that the surface soil layer would reach high moisture content values very rapidly. With this presumption, it limited the amount of water on the field, as well as the average period of a downpour under consideration, the duration of every experiment is limited to 10 min. If the moisture content of the tested soil is high (close to 20%), the time required for the simulation is 10–20 min (Sangüesa et al. 2010). In a publication by Aerts et al. (2006) used for the determination of surface runoff and the possibilities of seed wash-out, the authors simulated the rainfall with a maximal intensity of 120 mm/h, in 10 min durations. Kavian et al. (2020) in their experiment of a mulch application for purposes of erosion protection in variable moisture, used a rainfall intensity of 50.0 mm/h over a 10 min time period.

A large number of pluviometers (225 of them, which cover 33.18%, or 0.75 m^2 of the total surface area) that were used for the calibration, give precise data about the intensity and rainfall uniformity during the experiment, especially considering the relatively small surface area. For the purposes of this research, the constructed simulator achieves a rainfall intensity of 102–114 mm/h, and a very high CU for the surface area, which varies between 92.23 and 93.70% (Table 1). Mhaske et al. (2019) achieved intensities of 65, 93, 112 and 148 mm/h for raindrop diameters of 1.0–5.0 mm, with the CU varying between 81 and 88%, relative to the intensity achieved. Sangüesa et al. (2010) achieved a maximum CU of 92% for their specific surface area of 1 m^2. In a review paper where they compared the functioning and efficiency of 13 small portable rain simulators, Iserloh et al. (2013) state that the CU values varied between 66.9 and 97.8%, and only three of the mentioned simulators achieved a greater value than the one presented in this research. As mentioned in a publication by Vergni et al. (2018), indicating a smaller sampling zone within the simulator area is necessary in order to achieve satisfactory uniformity values.

The results of the raindrop size determination when utilising the flour method have shown that the average raindrop diameter formed in the simulator at D_{50} was 1.2 mm. These diameters correspond to the diameters of naturally occurring raindrops (Kolić 1988; Ristić & Malošević 2011). Iserloh et al. (2012) achieved simulated raindrop diameters D_{50} between 1.0 and 1.5 mm. Also, in a research study by Kavian et al. (2019), with optimal pressure in the system, an average raindrop diameter D_{50} of 1.2 mm was achieved.

The kinetic energy of the raindrop values, calculated for a rain intensity of 114 mm/h, are Ke_h = 355.35 J per m^2/h or $Ke_{10\,min}$ = 59.23 J/m^2/10 min. The height of the simulated rain ($h \approx 0.5$ m) is not sufficient to achieve the terminal velocity of the raindrops, thus making the kinetic energy at the impact point significantly smaller than in a natural rain occurrence. According to Cerdà et al. (1997), simulated raindrops have a lower velocity when hitting the surface compared to natural rain. Iserloh et al. (2013) confirmed this and stated that the main reason was generally the small heights from which the drops fall. Torri et al. (1994) utilised a rain simulator with a rainfall intensity of 36 mm/h, and a raindrop kinetic energy of 550 J/m^2/h. For simulated intensities of 30, 50 and 70 mm/h, Boulange et al. (2019) achieved kinetic energy values of 257.7, 760.1, and 1645.2 J per m^2/h, respectively. The values accounted for 78.0% and 86.5% of the energy of a natural occurring rain of 50 and 70 mm/h intensity, respectively.

However, the kinetic energy of raindrops does not have high significance for the research in question, considering that during this experiment, the litter and humus layers are removed from the test surface. According to Kolić (1988) and Cao et al. (2015), forest vegetation and litter significantly decrease the kinetic energy of raindrops.

In order for the simulator in question to be successfully used in the field, it is necessary to provide wind protection, in order to achieve the conditions obtained during the calibration. Besides that, utilisation of this type of system is not recommended on slopes greater than 15°.

CONCLUSION

The simulator described herein fully corresponds to all of the mentioned criteria for experimental research purposes. With an achieved rainfall intensity of 1.7–1.9 mm/min and a raindrop diameter of 1.2 mm, it corresponds to the described natural conditions of the research area. With its dimensions and construction design, it fulfils the criteria of portability during transport and simplicity during operation. Based on the measurements of the water consumption (47 L) and its losses (22.08%), it was

https://doi.org/10.17221/148/2021-SWR

determined that it fulfils the efficiency criterion. Based on the CU values that were achieved (92.23 to 93.70%), the spatial distribution of the raindrops and the homogeneity of the rainfall intensity were provided by the distribution of the sprayers while maintaining constant pressure.

The repeatability of the experiment under the same conditions was achieved by the construction design which provides the identical positioning of the sprayers during the apparatus installation, and by regulating and maintaining the pressure via a manometer, valves, and a pump throttle control. The marked sampling zone of the simulator area of 1.21 m^2 fulfils the requirements of the research that it was constructed for. The simulator was constructed out of easily available materials, thus proving itself to be feasible, with the total price not topping 500 euros.

REFERENCES

Abudi I., Carmi G., Berliner P. (2012): Rainfall simulator for field runoff studies. Journal of Hydrology, 454–455: 76–81.

Aerts R., Maes W., November E., Behailu M., Poesen J., Deckers J., Hermy M., Muys B. (2006): Surface runoff and seed trapping efficiency of shrubs in a regenerating semi-arid woodland in northern Ethiopia. Catena, 65: 61–70.

Agassi M., Bradford J.M. (1999): Methodologies for interrill soil erosion studies. Soil and Tillage Research, 49: 277–287.

Blinkov I. (2015): Review and comparison of water erosion intensity in the Western Balkan and EU countries. Contributions, Section of Natural, Mathematical and Biotechnical Sciences, MASA, 36: 27–42.

Boix-Fayos C., Martínez-Mena M., Arnau-Rosalén E., Calvo-Cases A., Castillo V., Albaladejo J. (2006): Measuring soil erosion by field plots: Understanding the sources of variation. Earth-Science Reviews, 78: 267–285.

Borrelli P., Panagos P., Märker M., Modugno S., Schütt B. (2017): Assessment of the impacts of clear-cutting on soil loss by water erosion in Italian forests: First comprehensive monitoring and modelling approach. Catena, 149: 770–781.

Borrelli P., Robinson D.A., Panagos P., Lugato E., Yang J.E., Alewell C., Wuepper D., Montanarella L., Ballabio C. (2020): Land use and climate change impacts on global soil erosion by water (2015–2070). Proceedings of the National Academy of Sciences of the USA, 117: 21994–22001.

Boulange J., Malhat F., Jaikaew P., Nanko K., Watanabe H. (2019): Portable rainfall simulator for plot-scale investigation of rainfall-runoff, and transport of sediment and pollutants. International Journal of Sediment Research, 34: 38–47.

Boxel Van J.H. (1997): Numerical model for the fall speed of raindrops in a rainfall simulator. Proceedings of the Workshop on Wind and Water Erosion, 5: 77–85.

Bryan R.B. (1974): Water erosion by splash and wash and the erodibility of Albertan soils. Geografiska Annaler: Series A, Physical Geography, 56: 159–181.

Cao L., Liang Y., Wang Y., Lu H. (2015): Runoff and soil loss from *Pinus massoniana* forest in Southern China after simulated rainfall. Catena, 129: 1–8.

Cerdà A. (1999): Rain simulators and their application in geomorphology: State of the art. Cuadernos de Investigación Geográfica/Geographical Research Letters, 25: 45–84. (in Spanish)

Cerdà A., Ibáñez S., Calvo A. (1997): Design and operation of a small and portable rainfall simulator for rugged terrain. Soil Technology, 11: 163–170.

Christiansen J.E. (1942): Irrigation by sprinkling. University of California Agricultural Experiment Station Bulletin, 670: 124.

Clarke M.A., Walsh R.P.D. (2007): A portable rainfall simulator for field assessment of splash and slopewash in remote locations. Earth Surface Processes and Landforms, 32: 2052–2069.

Corona R., Wilson T., D'Adderio L.P., Porcù F., Montaldo N., Albertson J. (2013): On the estimation of surface runoff through a new plot scale rainfall simulator in Sardinia, Italy. Procedia Environmental Sciences, 19: 875–884.

Dong J., Zhang K., Guo Z. (2012): Runoff and soil erosion from highway construction spoil deposits: A rainfall simulation study. Transportation Research, Part D1: 8–14.

Dunkerley D. (2008): Rain event properties in nature and in rainfall simulation experiments: A comparative review with recommendations for increasingly systematic study and reporting. Hydrological Processes, 22: 4415–4435.

FAO (2011): Assessing Forest Degradation: Towards the Development of Globally Applicable Guidlines Forest Resources Assessment. Forest Resources Assessment Working Paper 177. Rome, FAO.

Gabrić O. (2014): Experimental Research of Catchment Processes: Rainfall, Runoff and Soil Erosion. [Ph.D. Thesis.] Subotica, University of Novi Sad, Faculty of Civil Engineering.

Gavrilović S. (1972): Engineering of Torrents and Erosion. Journal of Construction (Special Issue). (in Serbian)

Guerra A.J.T., Fullen M.A., do Carmo M.O.J., Bezerra J.F.R., Shokr M.S. (2017): Slope processes, mass movement and soil erosion: A review. Pedosphere, 27: 27–41.

Guo W., Xu X., Zhu T., Zhang H., Wang W., Liu Y., Zhu M. (2020): Changes in particle size distribution of suspended sediment affected by gravity erosion: A field study

https://doi.org/10.17221/148/2021-SWR

on steep loess slopes. Journal of Soils and Sediments, 20: 1730–1741.

Holden J., Burt T.P. (2002): Infiltration, runoff and sediment production in blanket peat catchments: Implications of field rainfall simulation experiments. Hydrological Processes, 16: 2537–2557.

Hudson N. (1993): Field Measurement of Soil Erosion and Runoff. FAO Soils Bulletin No. 68, Rome, FAO.

Iserloh T., Fister W., Seeger M., Willger H., Ries J.B. (2012): A small portable rainfall simulator for reproducible experiments on soil erosion. Soil and Tillage Research, 124: 131–37.

Iserloh T., Ries J.B., Arnáez J., Boix-Fayos C., Butzen V., Cerdà A., Echeverría M.T., Fernández-Gálvez J., Fister W., Geißler C., Gómez J.A., Gómez-Macpherson H., Kuhn N.J., Lázaro, R., León F.J., Martínez-Mena M., Martínez-Murillo J.F., Marzen M., Mingorance M.D., Ortigosa L., Peters P., Regüés D., Ruiz-Sinoga J.D., Scholten T., Seeger M., Solé-Benet A., Wengel R., Wirtz S. (2013): European small portable rainfall simulators: A comparison of rainfall characteristics. Catena, 110: 100–112.

Jevtić Lj. (1978): Engineering Handbook for Torrent and Erosion Control. Belgrade, University of Belgrade, Faculty of Forestry. (in Serbian)

Jevtić Lj (1988): Torrent Hydrology. Belgrade, University of Belgrade, Faculty of Forestry. (in Serbian)

Johansen M.P., Hakonson T.E., Breshears D.D. (2001): Post-fire runoff and erosion from rainfall simulation: Contrasting forests with shrublands and grasslands. Hydrological Processes, 15: 2953–2965.

Kašanin-Grubin M., Hukić E., Bellan M., Bialek K., Bosela M., Coll L., Czacharowski M., Gajica G., Giammarchi F., Gömöryová E., del Rio M., Dinca L., Đogo Mračević S., Klopčić M., Mitrović S., Pach M., Randjelović D., Ruiz-Peinado R., Skrzyszewski J., Orlić J., Štrbac S., Stojadinović S., Tonon G., Tosti T., Uhl E., Veselinović G., Veselinović M., Zlatanov T., Tognetti R. (2021): Soil erodibility in European mountain beech forests. Canadian Journal of Forest Research, 51: 1846–1855.

Kathiravelu G., Lucke T., Nichols P. (2016): Rain drop measurement techniques: A review. Water, 8: 29.

Kavian A., Mohammadi M., Cerdà A., Fallah M., Gholami L. (2019): Design, manufacture and calibration of the SARI portable rainfall simulator for field and laboratory experiments. Hydrological Sciences Journal, 64: 350–360.

Kavian A., Kalehhouei M., Gholami L., Jafarian Z., Mohammadi M., Rodrigo-Comino J. (2020): The use of straw mulches to mitigate soil erosion under different antecedent soil moistures. Water, 12: 2518.

Kolić B. (1988): Forestry Ecoclimatology. Belgrade, Naučna knjiga/Scientific Book. (in Serbian)

Konz N., Baenninger D., Konz M., Nearing M., Alewell C. (2010): Process identification of soil erosion in steep mountain regions. Hydrology and Earth System Sciences, 14: 675–686.

Lora M., Camporese M., Salandin P. (2016): Design and performance of a nozzle-type rainfall simulator for landslide triggering experiments. Catena, 140: 77–89.

Meshesha D.T., Tsunekawa A., Haregeweyn N. (2019): Influence of raindrop size on rainfall intensity, kinetic energy, and erosivity in a sub-humid tropical area: A case study in the northern highlands of Ethiopia. Theoretical and Applied Climatology, 136: 1221–1231.

Meyer L.D., Harmon W.C. (1979): Multiple-intensity rainfall simulator for erosion research on row sideslopes. Transactions of the ASAE, 22: 0100–0103.

Mhaske S.N., Pathak K., Basak A. (2019): A comprehensive design of rainfall simulator for the assessment of soil erosion in the laboratory. Catena, 172: 408–420.

Milosavljević K (1949): Heavy rains and showers in Belgrade. Glasnik Srpskog Geografskog Društva/Bulletin of Serbian Geographical Society, 29: 13–21. (In Serbian)

Misra R.K., Rose C.W. (1995): An examination of the relationship between erodibility parameters and soil strength. Soil Research, 33: 715–732.

Montanarella L., Pennock D.J., McKenzie N., Badraoui M., Chude V., Baptista I., Mamo T., Yemefack M., Singh A.M., Yagi K., Young H.S., Vijarnsorn P., Zhang G.L., Arrouays D., Black H., Krasilnikov P., Sobocká J., Alegre J., Henriquez C.R., Mendonca Santos L.M., Taboada M., Espinosa-Victoria D., AlShankiti A., AlaviPanah S.K., Elsheikh E.A.E.M., Hempel J., Camps Arbestain M., Nachtergaele F., Vargas R. (2016): World's soils are under threat. Soil, 2: 79–82.

Morgan R.P.C. (2009): Soil Erosion and Conservation. Hoboken, John Wiley and Sons.

Newesely C.G.L., Zimmerhofer W., Kohl B., Markart G., Tasser E., Tappeiner U. (2015): Rain simulation in patchy landscapes: Insights from a case study in the Central Alps. Catena, 127: 1–8.

Panagos P., Borrelli P., Poesen J., Ballabio C., Lugato E., Meusburger K., Alewell C. (2015): The new assessment of soil loss by water erosion in Europe. Environmental Science and Policy, 54: 438–447.

Parsakhoo A., Lotfalian M., Kavian A., Hoseini S.A., Demir M. (2012): Calibration of a Portable single nozzle rainfall simulator for soil erodibility study in Hyrcanian Forests. African Journal of Agricultural Research, 7: 3957–3963.

Poesen J. (2018): Soil erosion in the Anthropocene: Research needs. Earth Surface Processes and Landforms, 43: 64–84.

https://doi.org/10.17221/148/2021-SWR

Polovina S., Radić B., Ristić R., Kovačević J., Milčanović V., Živanović N. (2021): Soil Erosion Assessment and Prediction in Urban Landscapes: A New G2 Model Approach. Applied Sciences, 11: 4154.

Polyakov V., Stone J., Collins C.H., Nearing M.A., Paige G., Buono J., Gomez-Pond R.L. (2018): Rainfall simulation experiments in the southwestern USA using the walnut gulch rainfall simulator. Earth System Science Data, 10: 19–26.

Qiu Y., Wang X., Xie Z., Wang Y. (2021): Effects of gravel-sand mulch on the runoff, erosion, and nutrient losses in the Loess Plateau of north-western China under simulated rainfall. Soil and Water Research, 16: 22–28.

Radić Z. (1981): Modern Methods of Analysis of Water and Sediment Movement in Open Streams. Scientific Research Project. Belgrade, University of Belgrade, Faculty of Civil Engineering, Institute of Hydraulic Engineering. (In Serbian)

Radić Z.M., Pavlović D. (2015): Spatial Analysis of Heavy Rains of Short Duration in Serbia. In: Int. Conf. Achievements in Civil Engineering, Subotica, Apr 24, 2015: 641–649. (In Serbian)

Rauch W., De Toffol S. (2006): On the issue of trend and noise in the estimation of extreme rainfall properties. Water Science and Technology, 54: 17–24.

RHSS (2014): Republic Hydrometeorological Services of Serbia, Extraordinary Climatological Bulletin Precipitation. Available at http://www.hidmet.gov.rs/index_eng.php (accessed Feb 15, 2021). (in Serbian)

Ristić R., Malošević D. (2011): Torrent Hydrology. Belgrade, University of Belgrade, Faculty of Forestry. (in Serbian)

Sangüesa C., Arumí J., Pizarro R., Link O. (2010): A rainfall simulator for the in situ study of superficial. Chilean Journal of Agricultural Research, 70: 178–182.

Singh H.V., Thompson A.M. (2016): Effect of antecedent soil moisture content on soil critical shear stress in agricultural watersheds. Geoderma, 262: 165–173.

Torri D., Colica A., Rockwell D. (1994): Preliminary study of the erosion mechanisms in a Biancana Badland (Tuscany, Italy). Catena, 23: 281–294.

Vergni L., Todisco F., Vinci A. (2018): Setup and calibration of the rainfall simulator of the masse experimental station for soil erosion studies. Catena, 167: 448–455.

Wilson T.G., Cortis C., Montaldo N., Albertson J.D. (2014): Development and testing of a large, transportable rainfall simulator for plot-scale runoff and parameter estimation. Hydrology and Earth System Sciences, 18: 4169–4183.

Yakubu M.L., Yusop Z. (2017): Adaptability of rainfall simulators as a research tool on urban sealed surfaces – a Review. Hydrological Sciences Journal, 62: 996–1012.

Zemke J.J. (2016): Runoff and soil erosion assessment on forest roads using a small scale rainfall simulator. Hydrology. 3: 25.

Zemke J.J., Enderling M., Klein A., Skubski M. (2019): The influence of soil compaction on runoff formation. A case study focusing on skid trails at forested Andosol sites. Geosciences, 9: 204.

Zhang K., Yu Y., Dong J., Yang Q., Xu X. (2019a): Adapting & Testing use of USLE K factor for agricultural soils in China. Agriculture, Ecosystems & Environment, 269: 148–55.

Zhang Y., Li X., Zhang X., Li H. (2019b): Investigating rainfall duration effects on transport of chemicals from soil to surface runoff on a loess slope under artificial rainfall conditions. Soil and Water Research, 14: 183–194.

Received: November 20, 2021
Accepted: March 28, 2022
Online first: April 26, 2022